

Accelerate Your CNN from Three Dimensions: A Comprehensive Pruning Framework

Wenxiao Wang¹, Minghao Chen¹, Shuai Zhao², Jinming Hu¹, Boxi Wu¹, Zhengxu Yu¹, Deng Cai¹, Haifeng Liu¹

¹ State Key Lab of CAD&CG, Zhejiang University

² The Chinese University of HongKong, Shenzhen

Abstract

To deploy a pre-trained deep CNN on resource-constrained mobile devices, neural network pruning is often used to cut down the model’s computational cost. For example, filter-level pruning (reducing the model’s width) or layer-level pruning (reducing the model’s depth) can both save computations with some sacrifice of accuracy. Besides, reducing the resolution of input images can also reach the same goal. Most previous methods focus on reducing one or two of these dimensions (i.e., depth, width, and image resolution) for acceleration. However, excessive reduction of any single dimension will lead to unacceptable accuracy loss, and we have to prune these three dimensions comprehensively to yield the best result. In this paper, a simple yet effective pruning framework is proposed to comprehensively consider these three dimensions. Our framework falls into two steps: 1) *Determining the optimal depth (d^*), width (w^*), and image resolution (r^*) for the model.* 2) *Pruning the model in terms of (d^* , w^* , r^*).* Specifically, in the first step, we formulate model acceleration as an optimization problem. It takes depth (d), width (w) and image resolution (r) as variables, and the model’s accuracy as the optimization objective. Although it is hard to determine the expression of the objective function, approximating it with polynomials is still feasible, during which several properties of the objective function are utilized to ease and speed up the fitting process. Then the optimal d^* , w^* , and r^* are attained by maximizing the objective function with Lagrange multiplier theorem and KKT conditions. Extensive experiments are done on several popular architectures and datasets. The results show that we have outperformed state-of-the-art pruning methods. The code will be published soon.

Introduction

CNN has achieved great success in many computer vision tasks such as image classification (He et al. 2016; Huang et al. 2017), object detection (Liu et al. 2016; Redmon et al. 2016), and semantic segmentation (Chen et al. 2017; He et al. 2017). However, the enormous computational cost of CNNs incapacitates them to be deployed on resource-constrained mobile devices such as smartphones. This gives birth to model acceleration (He et al. 2019; Zhou et al. 2018; Ba and Caruana 2014; He et al. 2018), a research field focusing on reducing the computational cost of models and

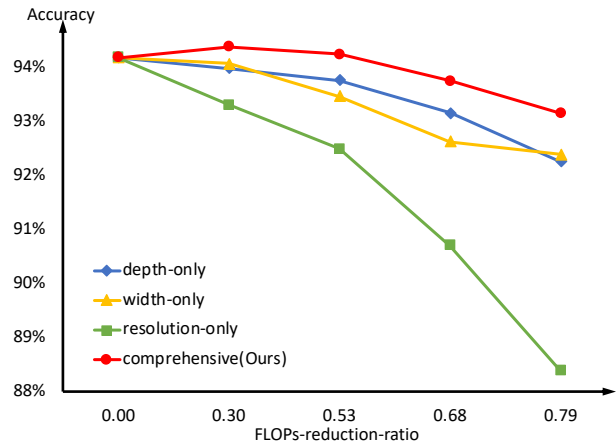


Figure 1: Accuracy of models with different pruning policies on CIFAR-10. The base model is ResNet56 (FLOPs-reduction-ratio = 0). X -only means the model is only pruned along X dimension, and “comprehensive” means three dimensions are pruned simultaneously. Larger FLOPs-reduction-ratio indicates a higher acceleration ratio.

keeping their performance at the same time for mobile deployment.

Neural network pruning is one of the most popular methods for model acceleration. It prunes redundant components of CNNs to cut down unessential computations. For example, filter-level pruning (He et al. 2019; Molchanov et al. 2017; Wang et al. 2019a; Luo et al. 2019; Liu et al. 2017) removes redundant filters and reduces the width of CNNs; Layer-level pruning (Wang et al. 2019b) removes unimportant layers and reduces the depth of CNNs. Besides, some methods (Howard et al. 2017), though less common, also turn to using resized low-resolution input images for fewer computations¹. These three kinds of methods respectively focus on one dimension (i.e., depth, width, and image resolution) that determines the computational cost of a model.

Naturally, we raise a question: given a pre-trained model, which dimension should we prune to minimize the model’s

¹Though images are actually resized for acceleration, we will use term “pruning images” for simplicity in the following.

accuracy loss? In practice, users empirically choose the most redundant dimension to prune, which often leads to a sub-optimal pruned model because of an inappropriate dimension choice. Worse, excessive pruning of any of these three dimensions will lead to unacceptable loss, as shown in Fig. 1. Instead, comprehensively pruning these dimensions yields better results. However, there has not been any effective method to achieve this. Though some previous methods can reduce the depth and width of the model simultaneously, the same methods are not applicable when considering image resolution². Motivated by (Tan and Le 2019), the optimal values for these dimensions can also be observed in a brute-force manner, i.e., grid search. However, grid search is costly (over 500 GPU³ hours for pruning ResNet for CIFAR-10) and often sub-optimal (if grid size > 1).

In this paper, we propose a pruning framework that prunes three dimensions comprehensively with acceptable time-consumption. Our framework falls into two steps:

Step 1: Determining Optimal d^*, w^*, r^* . Given a pre-trained model, we formulate model acceleration as an optimization problem: It takes depth (d), width (w), and resolution (r) as variables and maximizes the model’s accuracy (a) under the constraint of the computational cost; formally:

$$\max_{d,w,r} a = f(d, w, r), \text{ s.t. } g(d, w, r) \leq \tau, \quad (1)$$

where f is a model accuracy predictor (MAP), g represents the computational cost of the model, and τ is a constant threshold. (Tan and Le 2019) has provided a reasonable form of g . Though the expression of the MAP is unknown, it can be approximated with polynomials according to Taylor’s theorem, i.e., taking $N(N \sim 10^2)$ groups of $(d_i, w_i, r_i, a_i), i \in [1, N]$ and fitting the MAP with polynomial regression. Then the optimal d^*, w^*, r^* can be attained by maximizing the MAP with Lagrange multiplier theorem and KKT conditions. However, attaining (d_i, w_i, r_i, a_i) is a time-consuming process of training hundreds of models. To save time and cost, we speed up the process from two aspects: **1)** We take some prior information of the MAP (e.g., non-negativity, monotonicity, separability, etc.) as restrictions when fitting it. This prior information restricts the feasible region of solutions, allowing us to approximate the MAP accurately with few groups of data ($N = 13$). **2)** Given a pre-trained model and its configuration (d_0, w_0, r_0, a_0) , we can prune the model and fine-tune it to get other groups of (d_i, w_i, r_i, a_i) quickly. Generally, getting a group of (d_i, w_i, r_i, a_i) by pruning and fine-tuning takes only about $\frac{1}{4}$ as much time as training a new model from scratch.

Step 2: Pruning and Fine-tuning with d^*, w^*, r^* . We prune the model to target depth (d^*) and width (w^*) with some layer-level pruning and filter-level pruning algorithms. Then the model is fine-tuned with images of size r^* . At this step, the simplest magnitude-based filter-level pruning (Liu et al. 2017) and discrimination-based layer-level

pruning (Wang et al. 2019b) are used for simplicity, though other pruning algorithms are still applicable.

It is worth highlighting our contributions as follows:

- We propose an effective pruning framework that maximizes the pruned model’s accuracy by comprehensively pruning three dimensions (depth, width, and image resolution) with acceptable time-consumption.
- We explore the relationships between depth, width, image resolution, and model’s accuracy. Further, an effective method is proposed to fit their relationships in a fast way without training too many models.
- Extensive experiments are done on different architectures and datasets. The results show that our algorithm performs better than state-of-the-art filter-level pruning and layer-level pruning algorithms.

Background and Related Works

Neural Network Pruning. Neural network pruning compresses CNNs by pruning unimportant weights, filters, or layers in models, and the model after pruning will be fine-tuned on the dataset to recover its accuracy. Most neural network pruning methods fall into three categories: weight-level, filter-level, and layer-level pruning. Weight-level (Han, Mao, and Dally 2016) pruning has been receiving less attention because it needs specific libraries for sparse matrix (e.g., cuSPARSE) to accelerate the inference. However, the support of these libraries on mobile devices is limited. Instead, the most dominant pruning method, filter-level pruning (He et al. 2019, 2018; Wang et al. 2019a) compresses models by removing unimportant filters in CNNs, which can directly reduce the number of parameters and computations for all devices. Most researches focus on how to find unimportant filters. For example, magnitude-based methods (Liu et al. 2017; Li et al. 2017; He et al. 2018; Molchanov et al. 2017) take the magnitude of weights or feature maps from some layers as the importance criterion and prune those with small magnitude. Other methods propose to observe unimportant filters through their geometric median (He et al. 2019), correlation (Wang et al. 2019a), reconstruction loss (Luo et al. 2019), Taylor expansion (Molchanov et al. 2017), and so on.

Multi-Dimension Pruning. To the best of our knowledge, there are two methods (Lin et al. 2019; Wen et al. 2016) pruning models both in filter-level and layer-level. Both of them train base models with extra regularization terms and induce sparsity into models. Then the unit (filter or layer) with much sparsity will be pruned with slight loss. However, the same method cannot be used for balancing image size because images do not contain trainable parameters, and there is no way to induce sparsity into images.

Model Scaling. Model scaling is a task for neural network architecture search (NAS), which scales up a searched small network for higher accuracy. EfficientNet (Tan and Le 2019) proposes to scale up three dimensions (model’s depth,

²Please see Background and Related Works for the reason

³GTX 1080Ti

model’s width, and image size) simultaneously for best performance. Further, a grid search like method is proposed in the paper. Though the grid search method can also be used for pruning, it either takes a very long time to get the pruned model or yield a sub-optimal result (if grid size > 1).

Algorithm

Definitions and Notations

We define the depth of a model M as the number of basic blocks (e.g., Conv-BN-Relu blocks, residual blocks, etc.) that M contains. For example, ResNet32 contains 15 residual blocks, so its depth is 15 ($\text{depth}(M) = 15$). The width represents the number of filters of a certain layer l ($\text{width}(M[l])$), and $\text{resolution}(M)$ indicates the resolution of M ’s input images. For simplicity, we define (d, w, r) of a model (M_i) as the normalized depth, width, and image resolution:

$$d_i = \frac{\text{depth}(M_i)}{\text{depth}(M_0)}, w_i = \frac{\text{width}(M_i[l])}{\text{width}(M_0[l])}, r_i = \frac{\text{resolution}(M_i)}{\text{resolution}(M_0)}, \quad (2)$$

where M_0 is the baseline model. For filter pruning, we restrict all layers to be pruned with the same ratio, so the w_i of a model has no concern with the choice of l . Further, for a pruning task, it is natural to yield: $d_i, w_i, r_i \in (0, 1]$ and $d_0 = w_0 = r_0 = 1$.

Overview

We propose a comprehensive pruning framework that prunes the model along three dimensions (i.e., depth, width, and image resolution) simultaneously. Our framework falls into two steps: Given a pre-trained model, for the first step, we determine the optimal (d^*, w^*, r^*) by solving an optimization problem. For the second step, the model is pruned to the optimal (d^*, w^*) and fine-tuned with the r^* -sized images. The total pipeline of our algorithm is concluded in Fig. 2.

Model Acceleration as Optimization

Given a CNN architecture, the model’s depth, width, and image resolution are three key aspects that affect both the model’s accuracy and its computational cost. Thus, we formulate model acceleration as the following problem:

$$\begin{aligned} d^*, w^*, r^* &= \arg \max_{d, w, r} f(d, w, r; \Omega) \\ \text{s.t. } g(d, w, r) &\leq T \times g(d_0, w_0, r_0), \end{aligned} \quad (3)$$

where f is a **model accuracy predictor (MAP)**, which takes depth, width, and resolution as input and outputs the model’s accuracy. The MAP’s parameters, Ω , differ for different architectures or datasets; (d_0, w_0, r_0) is the base model’s configuration. g represents the computational cost (i.e., FLOPs) of a model. $T \in (0, 1)$ is a manually set parameter, representing that the pruned model’s computational cost is T of the original model. Motivated by (Tan and Le 2019) that the computational cost of a model is proportional to d, w^2 , and r^2 ($g \propto dw^2r^2$), we re-define the computational cost constraint as the following:

$$dw^2r^2 \leq T \times d_0w_0^2r_0^2. \quad (4)$$

The optimal d^*, w^*, r^* can be found with Lagrange multiplier theorem and KKT conditions once the MAP’s expression is known. According to Taylor’s theorem, though it is hard to speculate the expression of the MAP, approaching it with polynomials is still feasible. Specifically, we can train N models with different (d, w, r) , attain their accuracy (a), and take these groups of $(d_i, w_i, r_i, a_i), i \in [1, N]$ to fit the MAP with polynomials. Generally speaking, the polynomials will fit better as N increases. However, it is a time-consuming process to train so many models. Thus, we propose a fast MAP fitting method to finish the step in a rapid way in the next section.

Fast MAP Fitting

We provide two basic ideas to speed up the fitting process: 1) providing some prior information about MAP’s properties so that we can fit it well even with few data points (a smaller N). 2) Accelerate the process of fetching each data point (i.e., (d_i, w_i, r_i, a_i)) by taking advantage of pruning and fine-tuning. The details are as follows:

According to its definition, some of MAP’s properties are transparent:

Non-negativity & Boundedness. The accuracy of the model ranges from zero to one, i.e., $0 \leq f(d, w, r) \leq 1$.

Monotonicity. Models with smaller images or width or depth yield smaller accuracy⁴, i.e.,

$$\begin{aligned} d_1 \leq d_2 &\iff f(d_1, w_1, r_1) \leq f(d_2, w_1, r_1) \\ w_1 \leq w_2 &\iff f(d_1, w_1, r_1) \leq f(d_1, w_2, r_1) \\ r_1 \leq r_2 &\iff f(d_1, w_1, r_1) \leq f(d_1, w_1, r_2) \end{aligned} \quad (5)$$

Further, we design some experiments where two dimensions (e.g., depth, resolution) are freezing and explore how the accuracy varies along with the last dimension (e.g., width). As a result, we find that the influences of these three dimensions on accuracy are independent of each other. Formally,

$$\begin{aligned} \frac{f(d_2, w_1, r_1)}{f(d_2, w_2, r_1)} &= \frac{f(d_2, w_1, r_2)}{f(d_2, w_2, r_2)} \\ \frac{f(d_1, w_1, r_1)}{f(d_2, w_1, r_1)} &= \frac{f(d_1, w_1, r_2)}{f(d_2, w_1, r_2)} \\ \frac{f(d_1, w_1, r_2)}{f(d_2, w_1, r_2)} &= \frac{f(d_1, w_2, r_2)}{f(d_2, w_2, r_2)} \end{aligned} \quad (6)$$

holds for all $\{(d, w, r) | d, w, r \neq 0\}$, which leads us to $f(d, w, r)$ ’s another property⁵:

⁴Degradation problem (He et al. 2016) is not considered for simplicity because nowadays models have solved this problem to some extent

⁵Please see our supplementary materials for experiments and derivation of all properties.

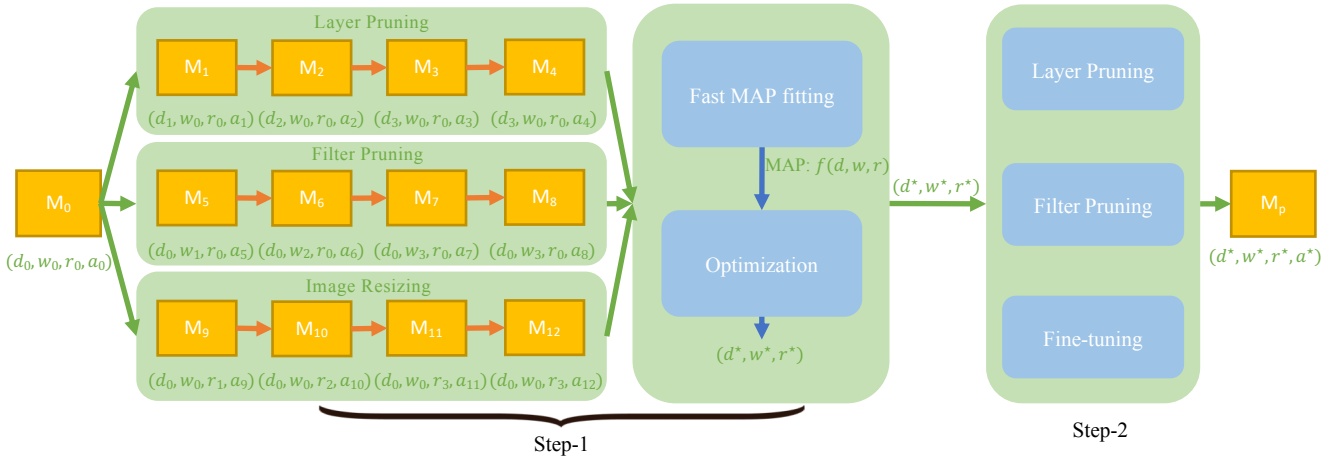


Figure 2: The pipeline of our pruning framework. At Step-1, pruning is done along three dimensions (depth, width and image resolution) independently, and several pruned models and their configurations (d_i, w_i, r_i, a_i) are attained. We take these configurations as training data and fit the MAP. Then the optimal d^*, w^* and r^* can be obtained by optimizing the MAP. At the Step-2, the model will be pruned and fine-tuned in terms of (d^*, w^*, r^*) .

Separability. Three variables in $f(d, w, r)$ are separable, i.e., $f(d, w, r)$ can be expressed in the form of:

$$f(d, w, r) = h_1(d) \times h_2(w) \times h_3(r). \quad (7)$$

Thanks to its separability, we can construct complex $f(d, w, r)$ by stacking unary polynomials $h_i(x; \Omega_i), i \in \{1, 2, 3\}$. Combined with the MAP's non-negativity and boundedness, we restrict $0 \leq h_i(x) \leq 1, i \in \{1, 2, 3\}$ without loss of generality. Moreover, it is easy to deduce that $h_i(x), i \in \{1, 2, 3\}$ are also monotonic increasing.

With this prior information, the MAP's fitting is reformulated as:

$$\begin{aligned} \arg \min_{\Omega} \sum_{n=1}^N (h_1(d_n) \times h_2(w_n) \times h_3(r_n) - a_n)^2 \\ \text{s.t. } 0 \leq h_i(x) \leq 1, i \in \{1, 2, 3\}, x \in [0, 1] \\ h'_i(x) \geq 0, i \in \{1, 2, 3\}, x \in [0, 1], \end{aligned} \quad (8)$$

where $h_i(x)$ is a unary polynomial:

$$h_i(x) = \sum_{j=0}^k \Omega_{ij} x^j, \Omega_{ij} \in \mathbb{R} \quad (9)$$

and k is the degree of h . The restrictions (prior information about MAP's properties) in Eq. 8 scale down the feasible region of solutions, allowing us to fit the MAP with fewer data points (a smaller N). Eq. 8 can be transformed as a semi-definite programming problem and solved easily.

Pruning for Fast MAP Fitting. We also take advantage of iterative pruning and fine-tuning to speed up fetching each group (d_i, w_i, r_i, a_i) . Precisely, given a pre-trained model M_0 and its configuration (d_0, w_0, r_0, a_0) , compared with training models from scratch, pruning and fine-tuning M_0

is a faster way to get the accuracy of models with different configurations. Here, we take pruning along width as an example: pruning redundant filters in M_0 from w_0 to $w_1 (w_1 < w_0)$ and fine-tuning the model yields M_1 as well as its configuration (d_0, w_1, r_0, a_1) . Similarly, pruning M_1 along width to $w_2 (w_2 < w_1)$ yields (d_0, w_2, r_0, a_2) . As the same rule, we can also prune the model along depth or fine-tune it with smaller images to attain other groups (d_i, w_i, r_i, a_i) .

Iterative pruning, rather than one-pass pruning, is used for two reasons: 1) Besides the final pruned model, iterative pruning yields several intermediate models as well as their configurations (d_i, w_i, r_i, a_i) , which can also be used for the MAP's fitting. 2) Compared with one-pass pruning, iterative pruning prunes fewer filters at each round, so it is possible to recover the model's accuracy with fewer fine-tuning epochs.

With the prior information for the MAP and the help of iterative pruning and fine-tuning, we can approach MAP with polynomials in a fast way.

Optimal Values for Three Dimensions

After getting the MAP, the optimal (d^*, w^*, r^*) of Eq. 3 can be solved easily. Specifically, according to KKT conditions, the inequality restrictions in Eq. 3 can be transformed into equality restrictions:

$$dw^2r^2 - T \times d_0w_0^2r_0^2 = 0, \quad (10)$$

and the solutions lie in Eq. 11 according to the Lagrange multiplier theorem, where λ is the Lagrange multiplier.

$$\begin{cases} dw^2r^2 - T \times d_0w_0^2r_0^2 = 0 \\ h'_1(d)h_2(w)h_3(r) + \lambda w^2r^2 = 0 \\ h_1(d)h'_2(w)h_3(r) + 2\lambda dwr^2 = 0 \\ h_1(d)h_2(w)h'_3(r) + 2\lambda dw^2r = 0 \end{cases} \quad (11)$$

Comprehensive Pruning and Fine-tuning

After attaining the optimal (d^*, w^*, r^*) , filter-level pruning and layer-level pruning methods are used to prune the model to target d^* and w^* , and then the model is fine-tuned with images of size r^* . During the pruning process, layer pruning first and filter pruning first are both viable and yield the same pruned model. Without loss of generality, we describe the process by assuming layer pruning first. Precisely, the steps are as follows:

Pruning Layers. Following DBP (Wang et al. 2019b), we put a linear classifier after each layer of model M_0 and test its accuracy on the evaluation dataset. The accuracy of each linear classifier indicates the discrimination of its corresponding layer’s features. Further, each layer’s discrimination enhancement compared with its preceding layer is seen as the importance of the layer. With this importance metric, we pick out the least important $(1 - d^*/d_0) \times 100\%$ layers and remove them from the M_0 , leading to a model M_{p1} .

Pruning Filters. The filter-level pruning is proceeded on M_{p1} . In particular, we use the scaling factor of BN layers as the importance metric, just like Slimming (Liu et al. 2017). However, different from Slimming that comparing the importance of all filters globally, we only compare the importance of filters in the same layer, and the least important $(1 - w^*/w_0) \times 100\%$ filters of each layer are pruned. With such modification, we keep all layers’ pruned ratios the same. Assuming the model after filter pruning is M_{p2} .

Fine-tuning with Smaller Images. After pruning, the pruned model M_{p2} is fine-tuned with images of size r^* . The images are resized to target size with the bilinear downsampling method, which is the most common downsampling for images. The model will be fine-tuned with a small learning rate till convergence, which leads to the final pruned model M_p .

Experiments

Experimental Settings

Datasets. Three popular datasets are used to check the performance of our algorithm: CIFAR-10 (Krizhevsky, Hinton et al. 2009), TinyImageNet (Wu, Zhang, and Xu 2017), and ImageNet (Russakovsky et al. 2015). These three datasets differ in their image-resolution (32×32 to 224×224), the number of classes (10 to 1000), and the scale of datasets (50k to 1000k images). For all datasets, images are augmented by symmetric padding, random clipping, and randomly horizontal flip, all of which are common (He et al. 2016; Wang et al. 2019a; Howard et al. 2017) augmentation methods for these datasets. The results show that our algorithm is well-generalized on different inputs.

Architectures. We also test our algorithm on several popular architectures: MobileNet (Howard et al. 2017), ResNet (He et al. 2016), and DenseNet (Huang et al. 2017). Their basic blocks vary from depth-separable convolution

Degree	Prior	#Train	#Eval	Mean Err(%)	Max Err(%)
3	×	80	20	0.53	1.65
4	×	80	20	0.29	0.58
5	×	80	20	0.14	0.35
6	×	80	20	0.16	0.31
7	×	80	20	0.10	0.29
10	×	80	20	0.09	0.33
5	×	13	20	0.36	0.76
5	✓	13	20	0.21	0.38
7	✓	13	20	0.19	0.36
10	✓	13	20	0.19	0.39

Table 1: Results of the MAP fitting. On hundred models with different (d, w, r) are trained. Each model’s accuracy (a) is the average of three independent trainings. These 100 groups of data are split into “Train” and “Eval” parts for polynomial fitting. The error is tested on “Eval” data. ‘#’ means “the number of”. “Prior” indicates whether to use our proposed prior information of the MAP for fitting.

blocks to residual and dense-connected blocks, representing three of the most popular designs for deep CNNs. Also, the results show the effectiveness of our algorithm across different architectures.

Evaluation Protocol. As other model acceleration methods do, we take the accuracy and FLOPs-reduction-ratio (Frr) as the evaluation protocol of our model acceleration algorithm. Formally, $Frr = 1 - \frac{FLOPs_p}{FLOPs_o}$, where $FLOPs_o$ and $FLOPs_p$ represent the floating-operations of the original model and the pruned model, respectively.

Compared Algorithms. The compared algorithms fall into four categories: fine-tuning the pre-trained model with smaller images, filter-level pruning, layer-level pruning, and pruning both filters and layers. In particular, the compared filter-level pruning algorithms are FPGM (He et al. 2019), PScratch (Wang et al. 2020), Slimming (Liu et al. 2017), Rethink (Liu et al. 2019), and HRank (Lin et al. 2020). As we know, there is only one algorithm, DBP (Wang et al. 2019b), focusing on layer-level pruning, which has also been compared. Further, GAL (Lin et al. 2019), which prunes filters and layers simultaneously, is also compared.

Training Settings. For base models training on CIFAR-10, we set the batch size to 64 for DenseNet and 128 for other architectures. Weight decay is set to $1e-4$. The models are trained for 160 epochs with the learning rate starting from 0.1 and divided by 10 at epoch 80 and 120. These are all the most common training settings (He et al. 2016; Wang et al. 2019a; Howard et al. 2017) for models for CIFAR-10. For all base models training on TinyImageNet and ImageNet, the batch size is set to 256, and weight decay is $1e-4$. All models are trained for 100 epochs.

Degree of Polynomials. Empirically, 5-degree unary polynomial is used for $h_i(x)$, $i \in [1, 3]$. However, experi-

Arch.	Alg.	Type	Acc.(%)	Frr.
MobileNet (93.50%)	r-only	I	86.77	0.75
	w-only	F	92.22	0.75
	Slimming	F	92.48	0.50
	PScratch	F	92.52	0.72
	DBP(d-only)	L	91.52	0.58
	GAL	F&L	91.94	0.75
	Ours	I&F&L	92.91	0.76
ResNet32 (93.18%)	r-only	I	90.19	0.52
	Slimming	F	92.08	0.50
	FPGM	F	92.14	0.53
	w-only	F	92.16	0.47
	PScratch	F	92.18	0.50
	DBP(d-only)	L	92.65	0.48
	Ours	I&F&L	92.95	0.50
ResNet56 (93.69%)	r-only	I	92.00	0.51
	w-only	F	92.97	0.50
	PScratch	F	93.05	0.50
	Rethink	F	93.07	0.50
	FPGM	F	93.35	0.50
	DBP(d-only)	L	93.27	0.52
	Ours	I&F&L	93.76	0.52
DenseNet40 (94.22%)	r-only	I	90.56	0.64
	HRank	F	93.64	0.41
	w-only	F	94.28	0.64
	Slimming	F	94.35	0.55
	DBP(d-only)	L	93.38	0.65
	GAL	F&L	93.53	0.55
	Ours	I&F&L	94.58	0.65

Table 2: Pruning Results on CIFAR-10. ‘F’, ‘L’, and ‘I’ mean filter-level pruning, layer-level pruning, and image re-sizing, respectively. “d-only”, “w-only” and “r-only” are the methods that our algorithm use, which have been introduced in the algorithm section.

ments in the ablation study show that pruning results are not so sensitive to the polynomial degree, and other choices (we test from 3-degree to 7-degree) also yield good results.

Data for Polynomial Fitting. Given a pre-trained model M_0 and its configuration (d_0, w_0, r_0, a_0) . All other data are extracted by reducing the size of one dimension. For example, according to Eq. 10, given a target T , the optimal depth must lie in the range $Td_0 \leq d^* \leq d_0$. Thus, we simplify M_0 iteratively to depth Td_0 through four times of layer pruning, which generates four groups of data, i.e., (d_i, w_0, r_0, a_i) , $i \in [1, 4]$, where $d_4 = Td_0$. Following the same rule, we can determine the range of w^* ($\sqrt{T}w_0 \leq w^* \leq w_0$) and r^* ($\sqrt{T}r_0 \leq r^* \leq r_0$). Similarly, by pruning M_0 on width or fine-tuning it with resized small images, other eight groups of data are attained. As a result, we approach the MAP with $N = 13$ groups of data, where (d_0, w_0, r_0, a_0) is included.

Pruning Settings. When attaining training data (i.e., (d_i, w_i, r_i) , $i \in [1, N]$) for polynomial fitting, all models on CIFAR-10 are fine-tuned for 40 epochs. Considering that

Arch.	Alg.	Type	Acc.(%)	Frr.
ResNet101 (64.83%)	r-only	I	55.48	0.75
	w-only	F	63.47	0.75
	FPGM	F	64.28	0.77
	Slimming	F	64.82	0.70
	DBP(d-only)	L	61.35	0.77
	GAL	F&L	64.33	0.76
	Ours	F&L&I	65.27	0.76
DenseNet100 (61.34%)	r-only	I	56.97	0.75
	FPGM	F	59.37	0.75
	w-only	F	59.56	0.75
	Slimming	F	59.63	0.74
	DBP(d-only)	L	58.44	0.77
	GAL	F&L	59.03	0.70
	Ours	F&L&I	60.22	0.75

Table 3: Pruning Results on TinyImageNet.

Arch.	Alg.	Type	Acc.(%)	Frr.
ResNet50 (76.15%)	r-only	I	71.56	0.50
	w-only	F	74.52	0.50
	FPGM	F	74.83	0.53
	PScratch	F	75.45	0.50
	DBP(d-only)	L	73.92	0.50
	GAL	F&L	72.95	0.43
	Ours	F&L&I	75.90	0.50

Table 4: Pruning Results on ImageNet.

12 models are attained, the process consumes as much time as training three models from scratch (because training one from scratch costs 160 epochs). At the final step, the model is fine-tuned for 80 epochs after pruning. The fine-tuning learning rate is set to $1e - 2$ at first and decays to $1e - 3$ at the half fine-tuning.

Results and Analysis

Results on MAP Fitting. We first design experiments to test the precision of polynomial fitting. In particular, ResNets with different depths (from ResNet8 to ResNet62) and widths (initial channels ranges from 8 to 16) are trained on CIFAR-10. Also, the resolution of images changes from 16 to 32. There are 100 different training settings, i.e., (d, w, r) . Each (d, w, r) is trained three times for the averaged accuracy (a) . Wherein, 80 data are for polynomial fitting, and others are for polynomial evaluation. Then we fit the relationship between (d, w, r) and a with polynomials of different degrees. The results are shown in Tab. 1. As we can see, polynomials over 4-degree all perform well in fitting with 80 training data. However, fitting with fewer data does entangle the problem, and even a 5-degree polynomial yields a 0.76% prediction error. Instead, using prior information about the MAP helps us approach the MAP accurately with only 13 groups data.

Results on CIFAR-10. Experiments on CIFAR-10 are done with ResNet and DenseNet. Several filter-level and layer-level pruning methods are compared. The results are shown in Tab. 2. As we can see, our method outperforms all

Degree	depth/ d^*	width/ w^*	resolution/ r^*	Acc.(%)	Frr.
3	22/0.80	14/0.86	29/0.95	92.98	0.50
4	21/0.76	13/0.83	32/1.00	93.78	0.49
5	20/0.74	14/0.85	32/1.00	93.79	0.49
6	22/0.80	13/0.82	31/0.98	93.50	0.48
7	19/0.72	14/0.88	32/1.00	93.69	0.50

Table 5: Pruning results with different degrees of polynomials. The baseline model is a ResNet56 (93.69%) pre-trained on CIFAR-10.

d	w	r	Frr.	Predicted(%)	Acc.(%)
1.00	1.00	1.00	-	-	93.69
0.90	0.93	1.00	0.25	93.62	93.66
0.84	0.95	1.00	0.25	93.55	93.79
1.00	0.95	0.95	0.26	93.53	93.70
0.90	1.00	0.92	0.27	93.44	93.68
0.87	0.93	0.95	0.25	93.42	93.60
0.45	0.80	0.95	0.75	92.55	92.63
0.50	0.80	0.90	0.75	92.44	92.56
0.55	0.80	0.85	0.75	92.30	92.43
0.65	0.65	0.95	0.74	91.93	92.00
0.70	0.80	0.75	0.75	91.87	91.89

Table 6: Pruning results on ResNet56 with CIFAR-10. Different (d, w, r) may yield similar results. ‘‘Predicted’’ means the predicted accuracy output by the MAP.

other pruning methods in a large margin. Notably, though the filter-level pruning method we use is a relatively naive one, we still overcome the state-of-the-art by pruning three dimensions comprehensively.

Results on TinyImageNet. TinyImageNet is much more complex than CIFAR-10. Thus, experiments are done with higher capacity CNNs, ResNet101, and DenseNet100. The results are shown in Tab. 3. As we can see, our algorithm outperforms others on accuracy with similar Frr .

Results on ImageNet. ImageNet contains about 1.28 million images consisting of 1000 classes. The images are of size 224×224 . The experiments are done on ResNet50. As we can see in Tab. 4, our algorithm achieves 0.45% higher accuracy than the state-of-the-art algorithm with higher Frr .

Ablation Study

Influence of Polynomials Degree. Though we have explored the influence of polynomials’ degree on the fitting error, it is still unknown whether different choices of polynomials’ degree will affect our pruning policy. Tab. 5 shows the results with different degrees. As we can see, 3-degree’s polynomial performs poorly in fitting MAP well. However, for polynomials with 4-degree or higher, they all predict the optimal depth, width, and image resolution well. Considering that the optimal depth, width, and image resolution are exactly what we want, we are disengaged from choosing the polynomial degree carefully.

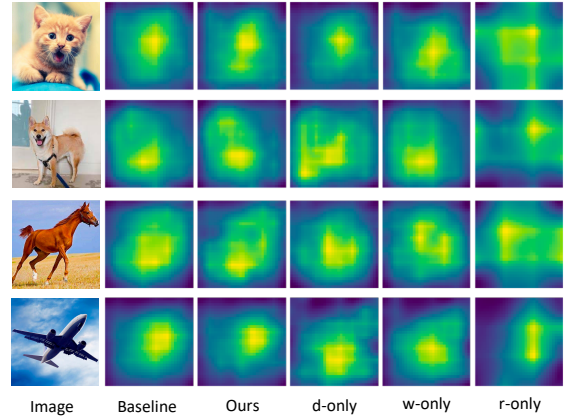


Figure 3: Visualizations of different models’ feature maps. The baseline model is a pre-trained ResNet56. Four different pruning policies are tested, and our pruned model’s feature maps look most like those of baseline models.

Case Study

Different Configurations, Similar Accuracy. We also find that different pruning policies may yield similar accuracy. In other words, the optimal depth, width, and image resolution may not be unique. As we can see in Tab. 6, with $Frr = 0.25$, reducing the width or the depth of ResNet56 yields similar accuracy. However, this phenomenon disappears when Frr becomes large. We presume the reason is that there is redundancy on both dimensions (depth and width) of the model. Pruning these redundant components (filters or layers) both induce slight loss. However, as Frr increases, the model becomes compact and more sensitive to the change of any dimension. Thus, our algorithm of pruning three dimensions comprehensively will show more significant advantages especially when Frr becomes larger.

Visualization of Feature Maps for Different Pruning Policies. In order to further understand why pruning three dimensions simultaneously yields better results than pruning one, Fig. 3 compares the feature maps for models with different pruning policies. All these models are pruned from the same baseline model, a ResNet56 pre-trained on CIFAR-10. Images are randomly chosen from the internet. As we can see, the feature maps that our pruned model outputs look most similar to those of the original model. This indicates that we preserve the most information of the original model by pruning three dimensions comprehensively.

Conclusion and Future Work

We propose a pruning framework that prunes three dimensions comprehensively. It first determines the optimal (d^*, w^*, r^*) by optimizing our proposed MAP and prunes models in terms of (d^*, w^*, r^*) . The results show that our algorithm outperforms state-of-the-art methods with similar computation cost by pruning three dimensions simultaneously. In the future, we will try to generalize our work to other computer vision tasks like objection detection, segmentation, etc.

References

- Ba, J.; and Caruana, R. 2014. Do Deep Nets Really Need to be Deep? In *NeurIPS*.
- Chen, L.; Papandreou, G.; Schroff, F.; and Adam, H. 2017. Rethinking Atrous Convolution for Semantic Image Segmentation. *CoRR* abs/1706.05587.
- Han, S.; Mao, H.; and Dally, W. J. 2016. Deep Compression: Compressing Deep Neural Network with Pruning, Trained Quantization and Huffman Coding. In Bengio, Y.; and LeCun, Y., eds., *4th International Conference on Learning Representations, ICLR 2016, San Juan, Puerto Rico, May 2-4, 2016, Conference Track Proceedings*. URL <http://arxiv.org/abs/1510.00149>.
- He, K.; Gkioxari, G.; Dollár, P.; and Girshick, R. B. 2017. Mask R-CNN. In *ICCV*.
- He, K.; Zhang, X.; Ren, S.; and Sun, J. 2016. Deep Residual Learning for Image Recognition. In *CVPR*.
- He, Y.; Kang, G.; Dong, X.; Fu, Y.; and Yang, Y. 2018. Soft Filter Pruning for Accelerating Deep Convolutional Neural Networks. In *IJCAI*.
- He, Y.; Liu, P.; Wang, Z.; Hu, Z.; and Yang, Y. 2019. Filter Pruning via Geometric Median for Deep Convolutional Neural Networks Acceleration. In *CVPR*.
- Howard, A. G.; Zhu, M.; Chen, B.; Kalenichenko, D.; Wang, W.; Weyand, T.; Andreetto, M.; and Adam, H. 2017. MobileNets: Efficient Convolutional Neural Networks for Mobile Vision Applications. *CoRR* abs/1704.04861.
- Huang, G.; Liu, Z.; van der Maaten, L.; and Weinberger, K. Q. 2017. Densely Connected Convolutional Networks. In *CVPR*.
- Krizhevsky, A.; Hinton, G.; et al. 2009. Learning multiple layers of features from tiny images. Technical report, Cite-seer.
- Li, H.; Kadav, A.; Durdanovic, I.; Samet, H.; and Graf, H. P. 2017. Pruning Filters for Efficient ConvNets. In *ICLR*.
- Lin, M.; Ji, R.; Wang, Y.; Zhang, Y.; Zhang, B.; Tian, Y.; and Shao, L. 2020. HRank: Filter Pruning Using High-Rank Feature Map. In *CVPR*.
- Lin, S.; Ji, R.; Yan, C.; Zhang, B.; Cao, L.; Ye, Q.; Huang, F.; and Doermann, D. S. 2019. Towards Optimal Structured CNN Pruning via Generative Adversarial Learning. In *CVPR*.
- Liu, W.; Anguelov, D.; Erhan, D.; Szegedy, C.; Reed, S. E.; Fu, C.; and Berg, A. C. 2016. SSD: Single Shot MultiBox Detector. In *ECCV*.
- Liu, Z.; Li, J.; Shen, Z.; Huang, G.; Yan, S.; and Zhang, C. 2017. Learning Efficient Convolutional Networks through Network Slimming. In *ICCV*.
- Liu, Z.; Sun, M.; Zhou, T.; Huang, G.; and Darrell, T. 2019. Rethinking the Value of Network Pruning. In *ICLR*.
- Luo, J.; Zhang, H.; Zhou, H.; Xie, C.; Wu, J.; and Lin, W. 2019. ThiNet: Pruning CNN Filters for a Thinner Net. *TPAMI*.
- Molchanov, P.; Tyree, S.; Karras, T.; Aila, T.; and Kautz, J. 2017. Pruning Convolutional Neural Networks for Resource Efficient Inference. In *ICLR*.
- Redmon, J.; Divvala, S. K.; Girshick, R. B.; and Farhadi, A. 2016. You Only Look Once: Unified, Real-Time Object Detection. In *CVPR*.
- Russakovsky, O.; Deng, J.; Su, H.; Krause, J.; Satheesh, S.; Ma, S.; Huang, Z.; Karpathy, A.; Khosla, A.; Bernstein, M. S.; Berg, A. C.; and Li, F. 2015. ImageNet Large Scale Visual Recognition Challenge. *IJCV*.
- Tan, M.; and Le, Q. V. 2019. EfficientNet: Rethinking Model Scaling for Convolutional Neural Networks. In *ICML*.
- Wang, W.; Fu, C.; Guo, J.; Cai, D.; and He, X. 2019a. COP: Customized Deep Model Compression via Regularized Correlation-Based Filter-Level Pruning. In *IJCAI*.
- Wang, W.; Zhao, S.; Chen, M.; Hu, J.; Cai, D.; and Liu, H. 2019b. DBP: Discrimination Based Block-Level Pruning for Deep Model Acceleration. *CoRR* abs/1912.10178.
- Wang, Y.; Zhang, X.; Xie, L.; Zhou, J.; Su, H.; Zhang, B.; and Hu, X. 2020. Pruning from Scratch. In *AAAI*.
- Wen, W.; Wu, C.; Wang, Y.; Chen, Y.; and Li, H. 2016. Learning Structured Sparsity in Deep Neural Networks. In Lee, D. D.; Sugiyama, M.; von Luxburg, U.; Guyon, I.; and Garnett, R., eds., *Advances in Neural Information Processing Systems 29: Annual Conference on Neural Information Processing Systems 2016, December 5-10, 2016, Barcelona, Spain, 2014–2082*. URL <http://papers.nips.cc/paper/6504-learning-structured-sparsity-in-deep-neural-networks>.
- Wu, J.; Zhang, Q.; and Xu, G. 2017. Tiny ImageNet Visual Recognition Challenge. Technical report.
- Zhou, G.; Fan, Y.; Cui, R.; Bian, W.; Zhu, X.; and Gai, K. 2018. Rocket Launching: A Universal and Efficient Framework for Training Well-Performing Light Net. In *AAAI*.